

Kalicy, G., Kumawat, H., Schwiening, J., Dzhygadlo, R., Gerhardt, A., Hohler, R., Lehmann, D., Lewandowski, B., Patsyuk, M., Peters, K., Schepers, G., Schmitt, L., Schwarz, C., Traxler, M., Zühlsdorf, M., Dodokhov, V. K., Vodopianov, A., Britting, A., Eyrich, W., Lehmann, A., Uhlig, F., Düren, M., Föhl, K., Hayrapetyan, A., Koch, P., Kröck, B., Merle, O., Cowie, E., Keri, T., Montgomery, R., Rosner, G., Seitz, B., Achenbach, P., Cardinali, M., Hoek, M., Sfienti, C., Thiel, M., Ugur, C., Bühler, P., Gruber, L., Marton, J., Suzuki, K., and Widmann, E. (2014) Status of the PANDA barrel DIRC. *Journal of Instrumentation*, 9, C05060.

Copyright © 2014 CERN.

This work is made available under the Creative Commons Attribution 3.0 Unported License (CC BY 3.0).

Version: Published

<http://eprints.gla.ac.uk/105853/>

Deposited on: 7 May 2015.

WORKSHOP ON FAST CHERENKOV DETECTORS - PHOTON DETECTION,
DIRC DESIGN AND DAQ
SEPTEMBER 4–6, 2013, GIESSEN, GERMANY

Status of the PANDA Barrel DIRC

G. Kalicy,^a H. Kumawat,^{a,1} J. Schwiening,^{a,2} R. Dzhygadlo,^a A. Gerhardt,^a
R. Hohler,^a D. Lehmann,^a B. Lewandowski,^a M. Patsyuk,^a K. Peters,^a G. Schepers,^a
L. Schmitt,^a C. Schwarz,^a M. Traxler,^a M. Zühlendorf,^a V. Kh. Dodokhov,^b
A. Vodopianov,^b A. Britting,^c W. Eyrich,^c A. Lehmann,^c F. Uhlig,^c M. Düren,^d
K. Föhl,^d A. Hayrapetyan,^d P. Koch,^d B. Kröck,^d O. Merle,^d E. Cowie,^e T. Keri,^e
R. Montgomery,^e G. Rosner,^e B. Seitz,^e P. Achenbach,^f M. Cardinali,^f M. Hoek,^f
C. Sfienti,^f M. Thiel,^f C. Ugur,^f P. Bühler,^g L. Gruber,^g J. Marton,^g K. Suzuki^g and
E. Widmann^g

The PANDA Cherenkov Group

^aGSI Helmholtzzentrum für Schwerionenforschung GmbH,
Darmstadt, Germany

^bJoint Institute for Nuclear Research,
Dubna, Russia

^cFriedrich Alexander Universität Erlangen-Nürnberg,
Erlangen-Nürnberg, Germany

^dII. Physikalisches Institut, Justus Liebig-Universität Gießen,
Gießen, Germany

^eUniversity of Glasgow,
Glasgow, United Kingdom

^fInstitut für Kernphysik, Johannes Gutenberg-Universität Mainz,
Mainz, Germany

^gStefan Meyer Institut für Subatomare Physik, Österreichische Akademie der Wissenschaften,
Wien, Austria

E-mail: J.Schwiening@gsi.de

ABSTRACT: The PANDA experiment at the future Facility for Antiproton and Ion Research in Europe GmbH (FAIR) at GSI, Darmstadt will study fundamental questions of hadron physics and QCD using high-intensity cooled antiproton beams with momenta between 1.5 and 15 GeV/c. Hadronic PID in the barrel region of the PANDA detector will be provided by a DIRC (Detection

¹Also at Bhabha Atomic Research Centre, Trombay, Mumbai, India

²Corresponding author.

of Internally Reflected Cherenkov light) counter. The design is based on the successful BABAR DIRC with several key improvements, such as fast photon timing and a compact imaging region. Detailed Monte Carlo simulation studies were performed for DIRC designs based on narrow bars or wide plates with a variety of focusing solutions. The performance of each design was characterized in terms of photon yield and single photon Cherenkov angle resolution and a maximum likelihood approach was used to determine the π/K separation. Selected design options were implemented in prototypes and tested with hadronic particle beams at GSI and CERN. This article describes the status of the design and R&D for the PANDA Barrel DIRC detector, with a focus on the performance of different DIRC designs in simulation and particle beams.

KEYWORDS: Cherenkov detectors; Cherenkov and transition radiation; Detector modelling and simulations I (interaction of radiation with matter, interaction of photons with matter, interaction of hadrons with matter, etc); Performance of High Energy Physics Detectors

Contents

1	Introduction	1
2	Barrel DIRC design	2
2.1	Baseline design	2
2.2	Design options	4
3	Simulation and reconstruction	5
4	Prototyping the PANDA Barrel DIRC	8
4.1	Component prototypes	9
4.2	System prototypes in particle beams	10
5	Conclusions	13

1 Introduction

Excellent charged Particle Identification (PID) over a large range of solid angle and particle momenta is essential to meet the physics objectives of the PANDA experiment [1] at the future FAIR facility at GSI. The complex physics program and the PID requirements for PANDA, as well as the PID systems covering particles in the forward region, are described in detail in ref. [2]. Charged hadron PID for the barrel section of the target spectrometer has to cover the angular range of 22-140° and needs to separate pions from kaons for momenta up to 3.5 GeV/c with a separation power of at least 3 standard deviations (s.d.). It has to operate in the $B \approx 2$ T magnetic field and at interaction rates up to 50MHz. Since the PID system is surrounded by an electromagnetic calorimeter, it should be thin in both radius and radiation length. All these requirements can be met by a Ring Imaging Cherenkov detector based on the DIRC (Detection of Internally Reflected Cherenkov light) principle.

A charged particle going through a solid radiator at a velocity faster than light in that medium emits Cherenkov photons on a cone with the half opening angle θ_C . This so-called Cherenkov angle is defined as $\cos\theta_C = 1/n(\lambda)\beta$, where $\beta=v/c$, v is the particle velocity, $n(\lambda)$ is the index of refraction of the material, which, in a dispersive medium, is a function of the wavelength (λ) of the Cherenkov photon. For a DIRC counter the radiator is typically a highly-polished rectangular narrow bar or wide plate made from synthetic fused silica with an average refractive index of $n=1.472$ at 380 nm. For $\beta \approx 1$ some of the photons will be caught inside the radiator due to total internal reflection and propagate towards the ends of the radiator. During those internal reflections the magnitude of the Cherenkov angle is preserved due to the high quality of the radiator surfaces. Photons propagating to the forward end are reflected by the mirror towards the readout end where they exit into an expansion volume and are imaged on a photodetector plane. The measured pixel

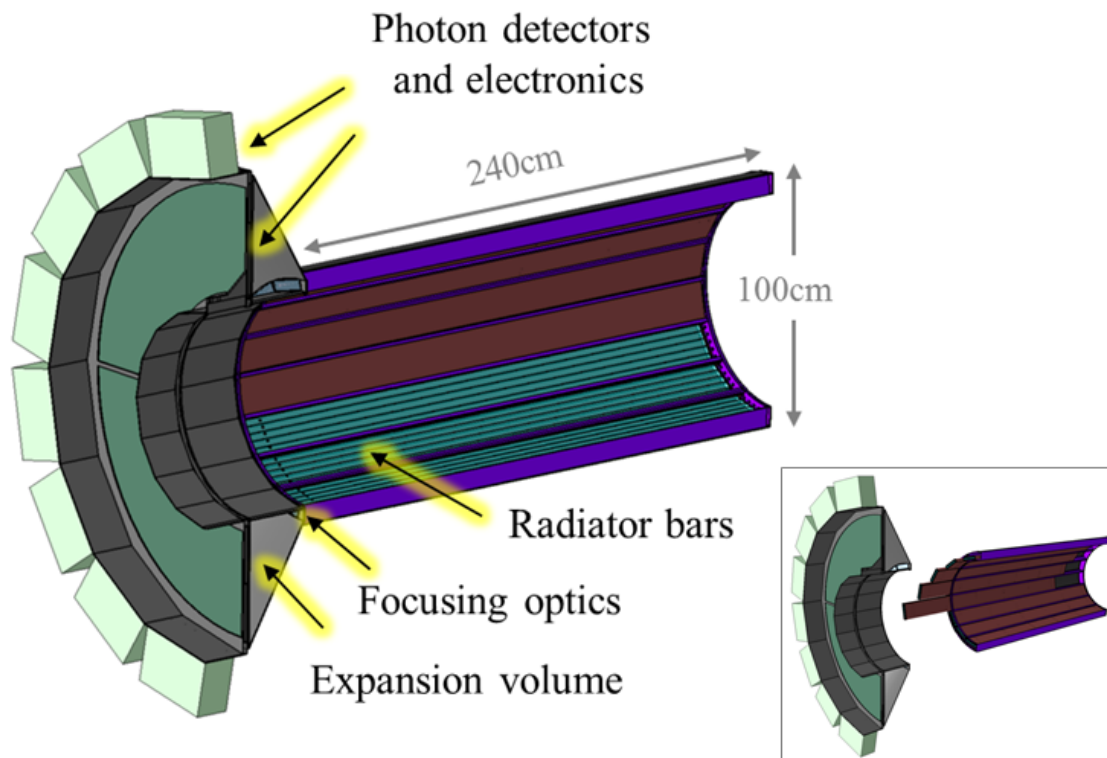


Figure 1. Schematic view of the PANDA Barrel DIRC baseline design. The insert illustrates the modular mechanical design concept.

coordinates and propagation time of each photon are combined with information from the tracking system (particle momentum and intersection point with the DIRC volume) to reconstruct the track Cherenkov angle and determine the corresponding PID likelihoods.

This article describes the PANDA Barrel DIRC design in section 2, followed by simulation studies of the performance of several design options in section 3. The Barrel DIRC prototyping program is described in section 4.

2 Barrel DIRC design

The PANDA Barrel DIRC design is inspired by the successful BABAR DIRC counter [3]. Some key improvements have been investigated to optimize the performance for PANDA. Focusing optics and fast timing are used to improve the resolution and a smaller expansion volume will decrease the sensitivity to accelerator-induced background and simplify the overall detector integration.

2.1 Baseline design

In the baseline design, shown schematically in figure 1, the radiators are narrow bars, made from synthetic fused silica, with a cross-section of $17\text{ mm} \times 32\text{ mm}$ and a length of 2400 mm, produced by gluing two 1200 mm-long pieces back-to-back.

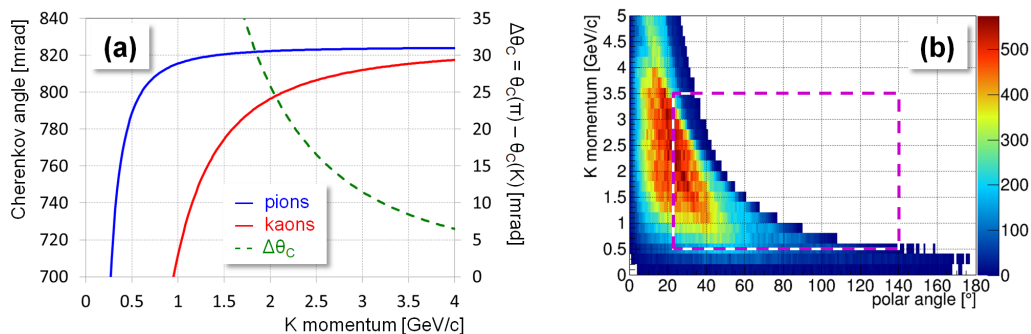


Figure 2. (a) Expected Cherenkov angle for pions and kaons as a function of particle momentum. (b) The pion/kaon Cherenkov angle difference, $\Delta(\theta_C)$, is shown as a dashed line. Phase space distribution of charged kaons in PANDA for a representative selection of physics channels requiring charged PID. The box indicates the range where the Barrel DIRC is expected to provide at least 3 s.d. π/K separation.

Five bars, placed side-by-side and separated by a small air gap, form one module, called a bar box. The bar boxes are arranged in a 16-sided polygonal barrel with a radius of 476 mm around the beam line. Mirrors are attached to the forward end of the bars to reflect the Cherenkov photons towards the readout end where they exit through a focusing lens and a window into a 30 cm-deep tank that serves as expansion volume (EV). The tank is filled with mineral oil to match the refractive index of the fused silica material and is equipped with entrance and exit windows. An array of Micro-Channel Plate Photomultiplier Tubes (MCP-PMTs) with a total of about 15,000 channels is placed at the EV backplane to measure the location and arrival time of the Cherenkov photons.

The mechanical design concept allows the entire readout unit, comprising the EV, electronics, and sensors, to be detached from the PANDA detector for access to the inner detectors. Each bar box is mounted on rails to slide into individual slots in the carbon fiber support structure to simplify installation.

The PID performance of a DIRC counter is driven by the track Cherenkov angle resolution σ_C defined as $\sigma_C^2 = \sigma_{C,\gamma}^2/N_\gamma + \sigma_{track}^2$, where N_γ is the number of detected photons and $\sigma_{C,\gamma}$ is the single photon Cherenkov angle resolution. σ_{track} is the uncertainty of the track direction in the DIRC, dominated by multiple scattering and the resolution of the PANDA tracking detectors. The single photon Cherenkov angle resolution (SPR) $\sigma_{C,\gamma}$ can be calculated as $\sigma_{C,\gamma}^2 = \sigma_{C,det}^2 + \sigma_{C,bar}^2 + \sigma_{C,trans}^2 + \sigma_{C,chrom}^2$ where $\sigma_{C,det}$ is the contribution from the detector pixel size, $\sigma_{C,bar}$ is the error due to optical aberration and imaging errors, $\sigma_{C,trans}$ is the error due to bar imperfections, such as non-squareness, and $\sigma_{C,chrom}$ is the uncertainty in the photon production angle due to the dispersion $n(\lambda)$ of the fused silica material.

The expected SPR of the Barrel DIRC baseline design is 8-9 mrad, dominated by a 6 mrad contribution from the size of the MCP-PMT pixels and about 5 mrad from chromatic dispersion.¹ The photon yield, defined as the number of detected Cherenkov photons, for a $\beta \approx 1$ particle is expected to be between 15 and 60, depending on the track angle. The resulting expected track Cherenkov angle resolution is $\sigma_C \approx 2$ –2.5 mrad, including a contribution of ≈ 2 mrad from the PANDA tracking system. The predicted π/K separation power can be calculated for any given momentum as

¹With precision photon timing at the level of 100 ps the chromatic error can be partially corrected [4].

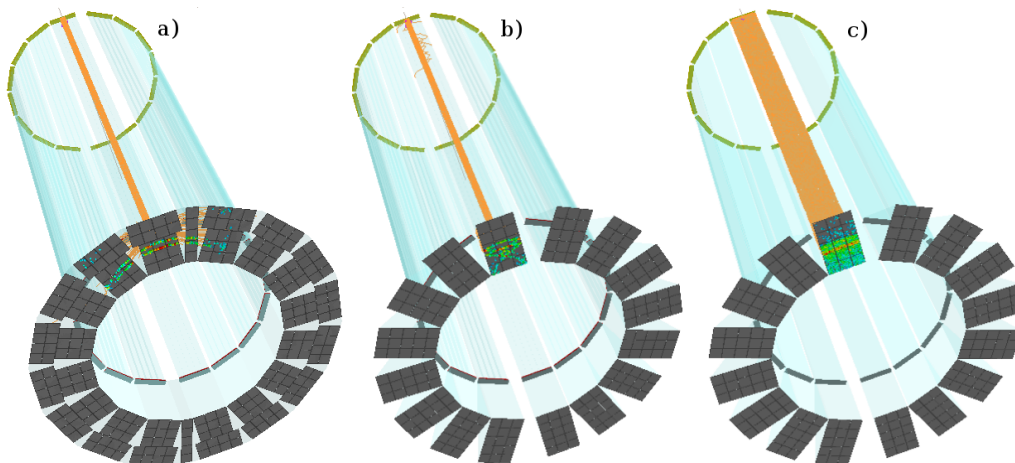


Figure 3. Geant simulation of a charged kaon in the PANDA Barrel DIRC for different radiator and expansion volume design options: a) narrow bars with an oil tank, b) narrow bars with compact prisms, c) wide plates with compact prisms. The kaon track, shown in grey, intersects the bar close to the mirror end. The Cherenkov photon trajectories are shown in orange. The accumulated hit pattern from 200 charged kaons is overlaid on the MCP-PMT detector plane.

$\Delta(\theta_C)/\sigma_C$, where $\Delta(\theta_C)$ is the momentum-dependent difference of the expected Cherenkov angle for pions and kaons, shown in figure 2a. At 3.5 GeV/c this angular difference is $\Delta(\theta_C) = 8.5$ mrad, resulting in an expected π/K separation power of 3 s.d. or more for the entire momentum range. Figure 2b shows that, due to the asymmetric interactions in PANDA, the highest kaon track momenta are observed in the forward direction. This is a good match to the performance of a Barrel DIRC, which is best for steep forward and backward angles where the photon yield is highest.

2.2 Design options

Several design options are being investigated for the Barrel DIRC components, including the size and shape of the expansion volume (EV) and the radiators, as shown in figure 3, and the type of focusing optics.

Two fundamentally different types of EV geometry are considered: a single 30 cm-deep tank filled with mineral oil or 16 individual compact prisms, also 30 cm deep, made from solid synthetic fused silica. The prisms reduce the number of MCP-PMTs required to cover the imaging plane and avoid the need for introducing mineral oil, a potential pollutant, to the inner part of the PANDA detector. Furthermore, although some mineral oils are a good match to the refractive index of fused silica [5], the superior optical quality of solid fused silica as EV material results in a significantly higher photon yield. However, such prisms are not only somewhat more expensive to fabricate than an oil tank but the sides of the prism add additional reflections to the photon path compared to the oil tank geometry, complicating both the hit patterns, as shown in figure 3, and the reconstruction of the Cherenkov angle.

The use of wide plates instead of narrow bars (figure 3c) would result in a significant reduction of the radiator fabrication cost since only 16 plates have to be built instead of 80 narrow bars. The Belle II TOP counter has demonstrated that high-quality wide plates can be fabricated by optical

industry [6]. However, a wide plate makes the use of a spherical focusing element impossible and requires a different reconstruction approach compared to narrow bars.

Due to the small size of the EV a focusing element is needed to obtain the desired Cherenkov angle resolution. Traditional singlet or doublet lenses require an air gap between the lens and the EV. However, a large fraction of the Cherenkov photons is reflected at the curved lens/air interface, leading to a loss of photons and a deterioration of the Cherenkov angle measurement. This effect is particularly important for those photons where the angle between the photon and the normal to the lens surface is large. This leads to the loss of up to 90% of the photons for particle track angles between 80° and 100° . Optimization of the optics in software using ZEMAX [7], standalone ray tracing and PANDARoot/Geant simulation [8] shows that a multi-component lens, using a material with a higher refractive index than fused silica, may offer a solution to the photon loss issue. A combination of N-LaK33 [9] (refractive index at 380nm $n=1.785$) and two layers of fused silica can provide the same refractive power at the N-LaK33/fused silica boundaries as a standard air gap lens with a much lower photon reflection probability. A prototype of such a high-refractive index compound lens has been built and tested in a Barrel DIRC prototype, described below. Since radiation hardness of the lens components is a concern, other high-refractive index materials are being studied as a possible alternative to N-LaK33.

3 Simulation and reconstruction

A detailed physical simulation of the PANDA Barrel DIRC was developed in the PANDARoot framework, which uses the Virtual Monte Carlo (VMC) approach to easily switch between Geant3 and Geant4 for systematic studies. The simulation is tuned to include measured values for the sensor quantum and collection efficiency, as well as timing resolution [10], the coefficient of total internal reflection of DIRC radiator bars as a function of photon energy [11], the bulk transmission of bars, glue, and lenses, and the reflectivity of the forward mirrors. Background from hadronic interactions and delta electrons is simulated as well as contributions from MCP-PMT dark noise and charge sharing between anode pads.

The reconstruction approach used for the baseline geometry with narrow bars is similar to the BABAR DIRC geometrical reconstruction. The known pixel position and bar location are used to define three-dimensional direction vectors between the center of the bar end and each pixel, which are stored in a look-up table (LUT). The LUT is generated from simulation by evenly illuminating the entire photodetector plane using a photon gun with a fixed wavelength, placed at the center of the bar end. This direction vector is then combined with the particle momentum, measured by the PANDA tracking system, to calculate the Cherenkov angle for each photon. The photon path from the track to the pixel is not unique and possible ambiguous path candidates, so-called solutions, add up to combinatorial background in the reconstruction. In addition to 8 solutions due to reflections inside the bar there are several possible solutions within the EV. Photons may propagate directly from the bar to the pixel or hit the top or bottom surface of the tank or prism. They may also be reflected once or several times from the sides of the prism before reaching the MCP-PMT. Each solution corresponds to a specific Cherenkov angle and, while the correct solutions contribute to a peak in a Cherenkov angle at the expected value, the incorrect solutions will form a combinatorial background. The measurement of the photon arrival time can be used to suppress this background

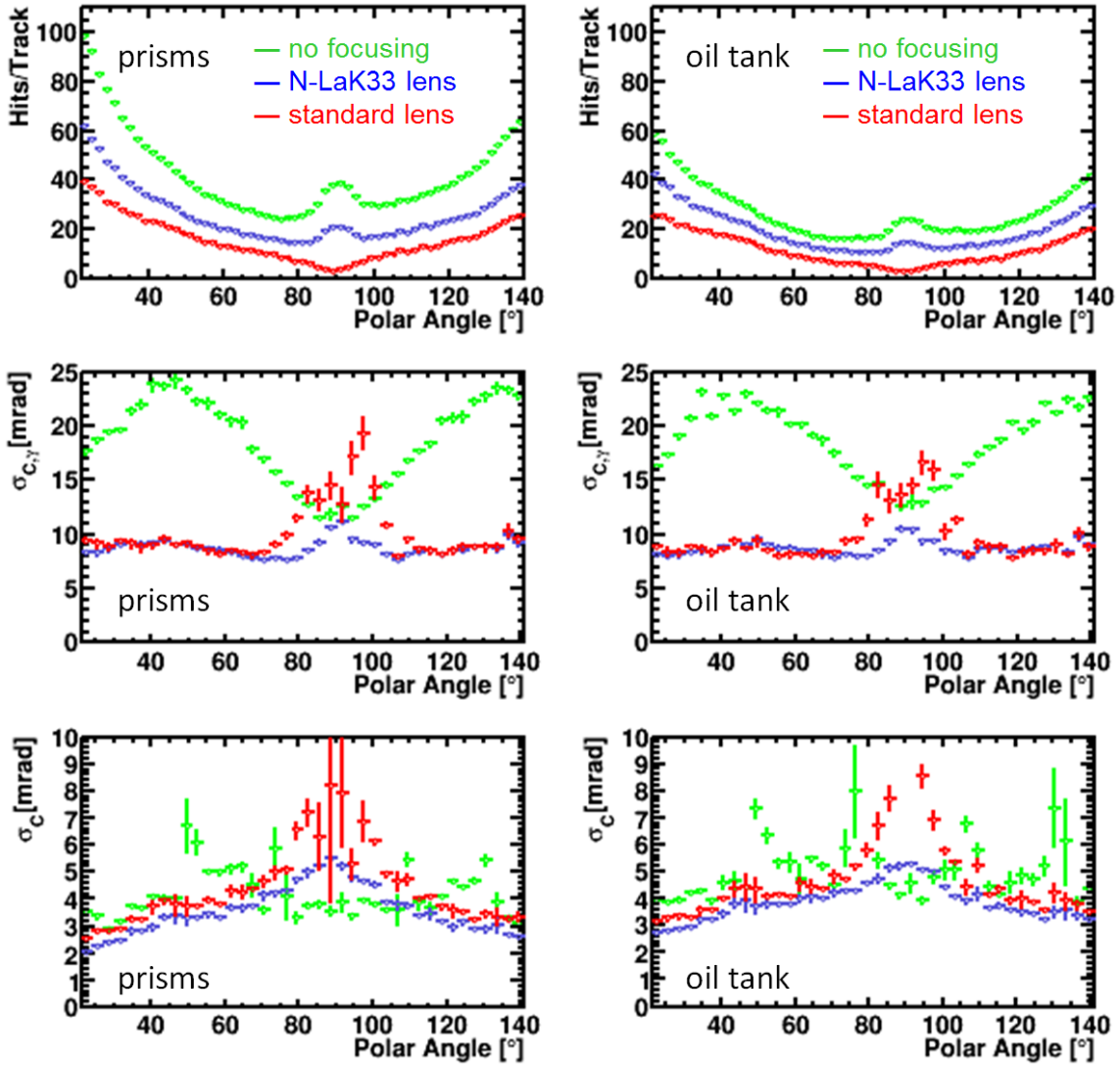


Figure 4. Reconstruction results for simulated 3.5 GeV/c muons for narrow bars in two EV configurations: compact prisms (left column) and oil tank (right column). The photon yield (top), single photon resolution (middle), and track Cherenkov angle resolution (bottom) are presented as a function of the polar angle for three focusing options. Results for the high-refractive index N-LaK33 lens without an air gap are shown in blue, for a standard lens with air gap in red. The configuration without focusing, where the bar is coupled directly to the prism, is shown in green.

by calculating a weight based on the difference between the measured photon propagation time and the time expected for a typical Cherenkov photon, taking the chromatic dispersion of the group velocity into account.

The track Cherenkov angle, θ_C , is determined by fitting a Gaussian plus linear background function to all solutions for a given particle, using a Maximum Likelihood approach. The difference between the expected Cherenkov angle per photon and the reconstructed value defines the single photon resolution ($\sigma_{C,\gamma}$) and the difference between the expected and reconstructed track Cherenkov angle is the track Cherenkov angle resolution.

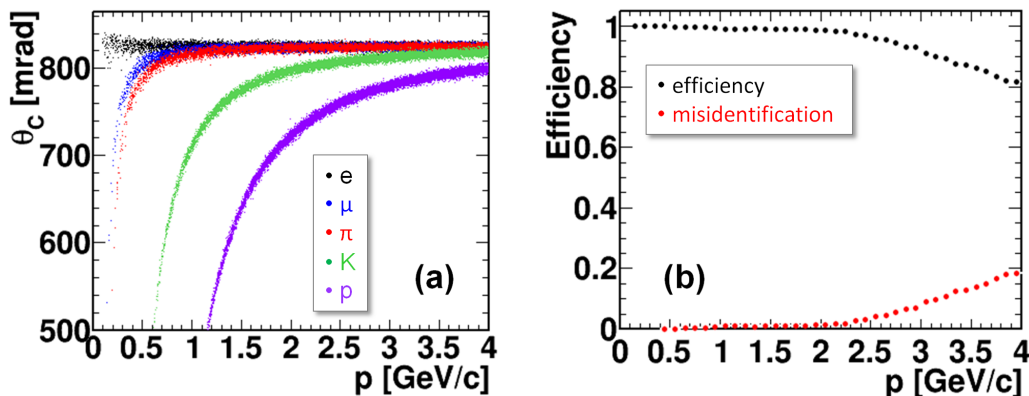


Figure 5. Reconstruction results for simulated e , μ , π , K , p for a geometry with narrow bars, standard spherical focusing lenses, and compact prisms. a) Reconstructed track Cherenkov angle and b) pion selection efficiency and mis-identification rate for a simple $3\sigma_C$ selection cut.

The performance of six geometries using narrow bars in combination with different EV and focusing options is compared in figure 4. The photon yield as well as the single photon and track Cherenkov angle resolution are shown as a function of the polar angle for a sample of muons with 3.5 GeV/c momentum, generated uniformly in azimuthal angle. Results are presented for the standard lens with air gap, for the high-refractive index lens, and for the bar coupled directly to the EV.

While the designs without focusing have a high photon yield of 30–100 photons for prisms and 20–60 photons for the oil tank, the poor single photon Cherenkov angle resolution of those designs leads to a track Cherenkov angle resolution significantly worse than the 2.8 mrad required for the 3 s.d. π/K separation. The two configurations with lenses reach a single photon resolution close to the design goal of 8–10 mrad except for angles of 80–100° where the combinatorial background from ambiguous photon paths between bar and pixel is most severe.

The lens with an air gap suffers from significant photon yield losses near 90° polar angle due to total internal reflection of the photons at the lens-air interface. This causes the Cherenkov angle resolution values to deteriorate. The small number of detected photons, fewer than 5 for 80–100°, makes the design very sensitive to track and event backgrounds, including Cherenkov photons from δ -electrons, γ -induced e^+e^- pairs, and neutrons, as well as back scattering from the electromagnetic calorimeter, which, according to simulation produce 5–10 background photons per track.

The prism EV with high-refractive index lens reaches the design goals in both the photon yield and the single photon resolution. The track Cherenkov angle resolution is below 2.5 mrad at the forward angles and considerably better than the 3 s.d. requirement for the entire angle range. Due to the asymmetric interactions in PANDA, where the higher momentum particles are produced predominantly in the forward direction, the 4–5 mrad track Cherenkov angle resolution in the 80–100° range is still better than required.

The Cherenkov angle per track from the maximum likelihood fit is shown in figure 5a for a sample of simulated particles in a geometry with a standard lens and a prism EV. A simple pion selection can then be performed based on the agreement of the Cherenkov angle with the expected value for pions and a separation of at least 3 s.d. from the expected angle for kaons or protons. The resulting efficiency for a simple selection of charged pions is shown, together with the

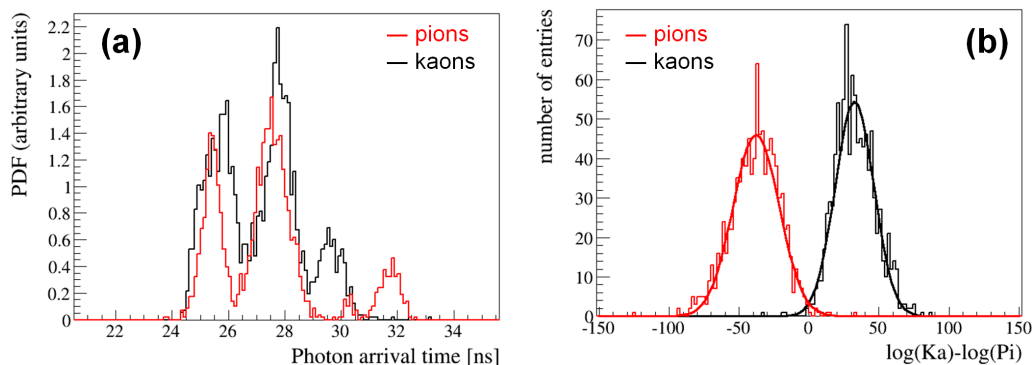


Figure 6. Examples for the time-based reconstruction of the plate geometry without a lens: Photon arrival time for charged pions and kaons for a selected MCP-PMT pixel (a) and log-likelihood difference for kaon and pion hypotheses (b) for a sample of 3.5 GeV/c pions and kaons at 22° polar angle and a single photon timing resolution of 100 ps.

mis-identification from kaons and protons, in figure 5b. The mis-identification rate of 10–15% at 3.5 GeV/c is consistent with the 3 s.d. PID requirement. Both the efficiency and mis-identification rate are expected to improve for a more sophisticated likelihood selector, which is currently being developed.

The geometric reconstruction approach using LUTs does not work for wide radiator plates since the assumption that the photons exit from the center of the radiator is no longer valid. Instead, a maximum likelihood method, based on the PID approach used for the Belle II time-of-propagation counter [12], is applied to compare for each track, pixel by pixel, the measured photon arrival time to the times expected for each particle hypothesis. The corresponding Probability Density Functions (PDF) are derived from the simulation and an example for one pixel is given in figure 6a. The time-based PDF is multiplied with a Poissonian PDF for the number of detected Cherenkov photons and the log-likelihood difference is calculated to perform the PID. Figure 6b shows the π/K log-likelihood difference for a sample of 3.5 GeV/c pions and kaons at 22° polar angle, the most challenging case for the PANDA Barrel DIRC, for a plate geometry without focusing optics. The separation power corresponds to more than 4 s.d., making the plate design an interesting option for PANDA although the influence of the non-Gaussian tails in the log-likelihood difference needs further studies. Studies of the performance of a wide plate in combination with a cylindrical high-refractive index compound lens are ongoing.

4 Prototyping the PANDA Barrel DIRC

While the simulation studies have identified several promising design options, decisions about the ultimate PANDA Barrel DIRC design can only be made after validating the performance in system prototypes using particle beams. Additional measurements on test benches, using electronic pulsers and lasers, are required to verify the performance of component prototypes, such as the photodetectors, readout electronics, or bars and plates from different manufacturers.

4.1 Component prototypes

One of the main technical challenges for the PANDA Barrel DIRC is the efficient detection of single photons with good resolution (100 ps or better in time and few mm in position) in the 1 T magnetic field at reaction rates up to 50 MHz. For many years the leading sensor candidate, MCP-PMTs, suffered from photocathode aging due to ion backflow, limiting the lifetime of MCP-PMTs to a few months of PANDA operations at full luminosity. Recent improvement in the MCP-PMT lifetime, described in ref. [10], identified two MCP-PMT models (PHOTONIS Planacon XP85112 and Hamamatsu SL-10) which meet or exceed all Barrel DIRC sensor specifications.

The data acquisition will be performed using the trigger and readout board (TRB) [13], originally developed for the HADES experiment. Development and tests of the latest version of the TRB and front-end boards for PANDA are described in detail in ref. [14]. The prototype tests in particle beams were performed with an earlier version of the TRB (version 2) in combination with an add-on board that performed signal discrimination using the NINO chip to measure the time using the CERN HPTDC [15].

The optical and mechanical quality of the DIRC radiator bars is of critical importance for the photon yield and single photon resolution and, thus, the PID performance. Depending on the particle polar angle Cherenkov photons are internally reflected up to 200 times before exiting the bar. The probability of photon loss during total internal reflection is determined by the surface roughness and sub-surface damage, created in the fabrication process. A transport efficiency of 90% requires a surface polish at the level of 5–10 Å. To maintain the magnitude of the Cherenkov angle during the reflections the bar surfaces have to be parallel and square to better than 0.25 mrad. The combination of these tight optical and mechanical specification makes the production of DIRC radiators challenging for the optical industry. During the PANDA Barrel DIRC prototyping program a total of about 30 bars and plates were produced by six manufactures, using different fabrication techniques. The quality of these prototypes was tested in three separate experimental setups.

Two setups measure the parallelism and squareness of the bar surfaces. One uses an auto-collimator, the other a laser reflected from the bar sides. The angular precision achieved is better than 0.1 mrad. Bars from several of the manufacturers were found to meet the angular specifications.

Another setup, shown in figure 7a, is installed in a dark, temperature-stabilized clean room to determine the coefficient of total internal reflection of a number of prototype radiators. The fraction of light transmitted after about 50 internal reflections in a bar is measured using several laser wavelengths and related to surface roughness via the scalar scattering theory [16]. Figure 7b shows the results from an earlier prototype bar for three different laser wavelengths compared to predictions from scalar theory and a scalar theory fit to the data, found to be in good agreement with manufacturer's data. The setup was recently upgraded to allow the measurement of longer bars, up to 2.5 m length, and to extend the laser wavelength into the UV range. This increases the sensitivity to subsurface damage, improves measurement accuracy, and allows a detailed comparison of the techniques used to produce prototype bars.

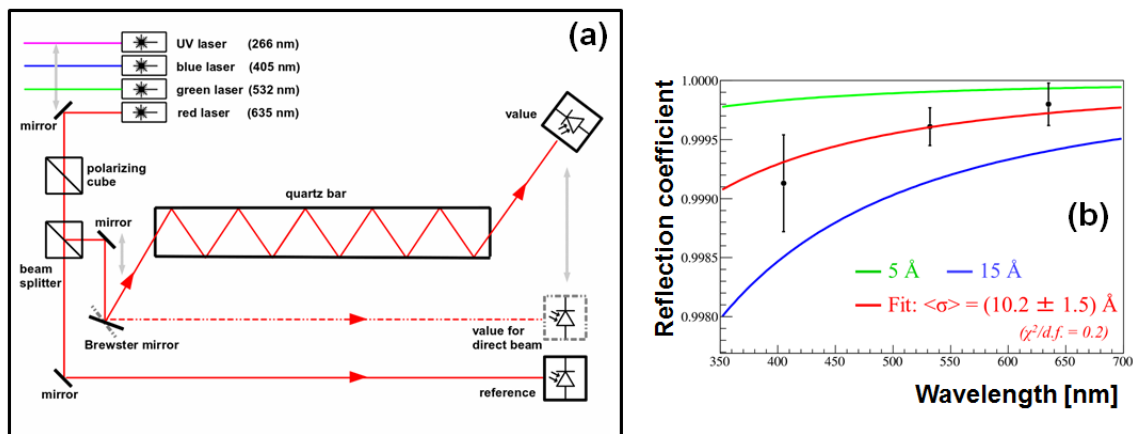


Figure 7. a) Schematic illustration of the setup used to measure the coefficient of total internal reflection of DIRC bars. b) Example of measurement results for a prototype bar with predictions from scalar theory and a fit to the data.

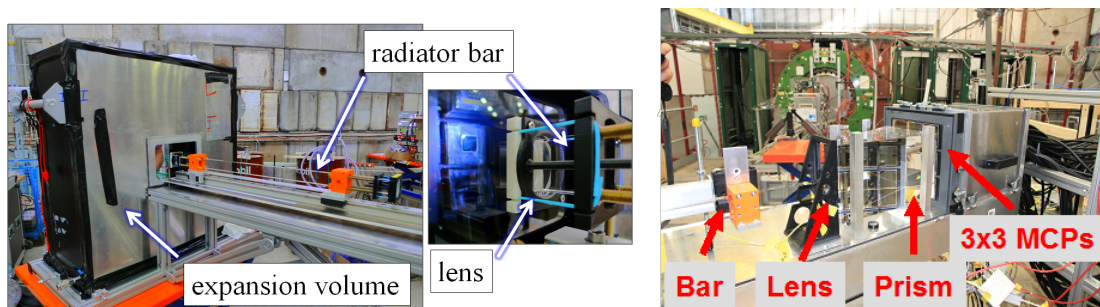


Figure 8. Photo of the Barrel DIRC prototype setup in 2011 (a) and 2012 (b) in the T9 beam line at CERN.

4.2 System prototypes in particle beams

All prototypes have several components in common: a dark box containing a radiator bar, an expansion volume, and a photodetector array connected to TRB-based readout electronics. These components, together with a focusing lens, formed the first prototype. It was tested with a proton beam at GSI in 2008 and 2009. The observed ring image and photon timing behavior provided the proof-of-principle for this focusing DIRC concept.

The second, more complex, prototype, shown in figure 8a, included a larger and deeper expansion volume and was mounted on a stage that could be moved and rotated relative to the particle beam. Focusing lenses with different Anti Reflective (AR) coatings were available and bars from different manufacturers could be tested. The expansion volume was an oil tank filled with Marcol mineral oil [17] and a variety of photodetectors, including MCP-PMTs, SiPM, and Multi-Anode PMT, could be placed on the large focal plane. The data collected from two campaigns in 2011, at GSI and at CERN, were used for the first determination of the Cherenkov angle resolution and the photon yield of the design using a narrow bar and an oil tank.

Several key design options were implemented in the third prototype and tested in the summer 2012 at CERN. A photo of the prototype components and a schematic view of the setup are shown

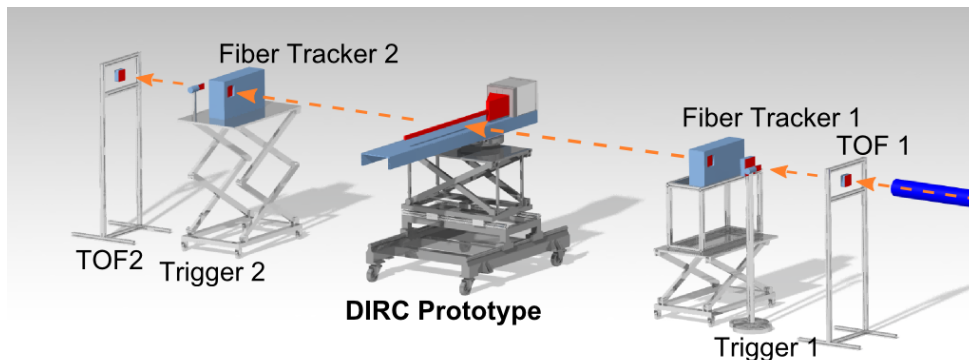


Figure 9. Schematic view of the prototype configuration at CERN in 2012.

in figures 8b and 9, respectively. A synthetic fused silica bar ($17 \times 35 \times 1225 \text{ mm}^3$) with a focusing lens attached to one end and a mirror to the other end was placed into a light-tight container. A large synthetic fused silica prism with a depth of 30 cm, located about 2 mm from the lens, served as expansion volume. The hit location and the photon propagation time of each photon were measured with an array of nine PHOTONIS XP85112 MCP-PMTs coupled with optical grease to the back surface of the prism. The data acquisition for 896 channels was performed using the TRB (version 2) boards.

The setup was placed into the mixed hadron beam at the T9 area of the CERN PS. A hadron-rich target was used to select positively charged particles with momenta ranging from 1.5 GeV/c to 10 GeV/c, depending on the prototype configuration. The trigger was provided by two scintillator counters and two scintillating fiber tracking stations measured the beam direction. A time-of-flight system was used for tagging pions and protons with momenta up to 6 GeV/c.

A total of about 220M triggers were recorded in several configurations. Spherical and cylindrical focusing lenses with and without anti-reflective coatings were available as well as a high-refractive index compound lens without an air gap. A number of narrow radiator bars made by different manufacturers from synthetic fused silica bar or acrylic glass, as well as a 17cm-wide synthetic fused silica plate, were tested to compare the Cherenkov angle resolution and photon yield.

The polar angle between the particle beam and the bar was varied between 20° and 156° , and the interception point between beam and bar was scanned 80 cm along the long bar axis covering the range similar to the PANDA phase space. An example of the occupancy plot for a 124° polar angle is shown in figure 10. Although the hit pattern is complicated with overlapping segments due to reflections from the top, bottom, and sides of the prism, these features are in good agreement with the prediction for 10 GeV/c pions, calculated from the ray-tracing simulation. The simulation contains much less background than the data because, in contrast to the full PANDA simulation in Geant, processes like δ -electrons, MCP-PMT dark noise or charge sharing are not included.

The reconstructed Cherenkov angle per photon for a prototype configuration with a narrow fused silica bar and a spherical lens with a 2 mm air gap between lens and prism is shown in figure 11a. The distribution shows large bin-to-bin fluctuations that are the result of the ring image being mostly parallel to MCP-PMT columns. This pixelization effect can be avoided by combining the data from runs at several different polar angles. The result of a combination of eight runs with

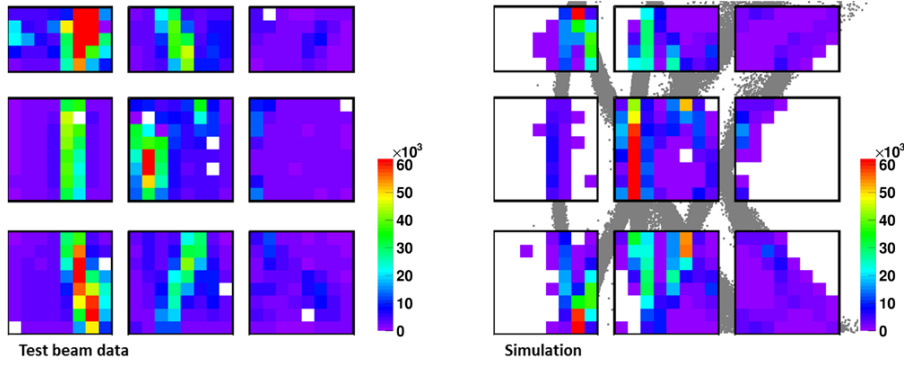


Figure 10. Number of detected photons per MCP-PMT pixel for about 200,000 triggers from the 2012 prototype at CERN (left) and the corresponding simulation (right). The hit position of individual Cherenkov photons between the MCP-PMTs in simulation is overlaid as points.

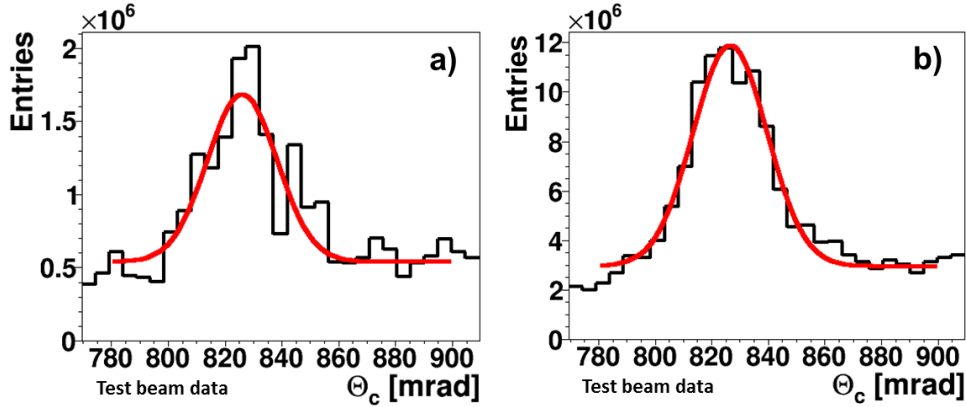


Figure 11. Reconstructed Cherenkov angle per photon from 2012 prototype data for a configuration using a standard lens with air gap. The distribution for a single run for a polar angle of 124° (a) demonstrates the pixelization effect which is smoothed out in the combination of 8 runs from the polar angle range $122\text{--}124^\circ$ (b). The mean and width of the fit to the distributions are $\Theta_C = 826.1 \text{ mrad}/\sigma_{C,\gamma} = 12.3 \text{ mrad}$ (a) and $\Theta_C = 826.3 \text{ mrad}/\sigma_{C,\gamma} = 13.0 \text{ mrad}$ (b).

polar angles between $122\text{--}124^\circ$ can be seen in figure 11b. A Gaussian with a linear background was fitted to the distribution and the resulting mean and width are consistent with simulation if the contribution from the beam divergence is taken into consideration.

The number of detected photons per track depends on the length of the particle track in the bar, which is a function of the track polar and azimuth angles, as well as on the optical quality of the radiator and the coupling between bar, lens, and prism. The location of the ring image on the MCP-PMT array is another important factor since part of the hit pattern is lost in the gaps between MCP-PMTs. The prediction of the ray-tracing simulation for the photon yield as a function of the track polar angle is shown for several lens configurations in figure 12a. The standard spherical UV lens with anti-reflective coating and a 2 mm air gap has an acceptable yield for most of the track angles compared to the cylindrical high-refractive index compound lens made from synthetic fused silica and N-LaK33 except for the range between $80\text{--}100^\circ$.

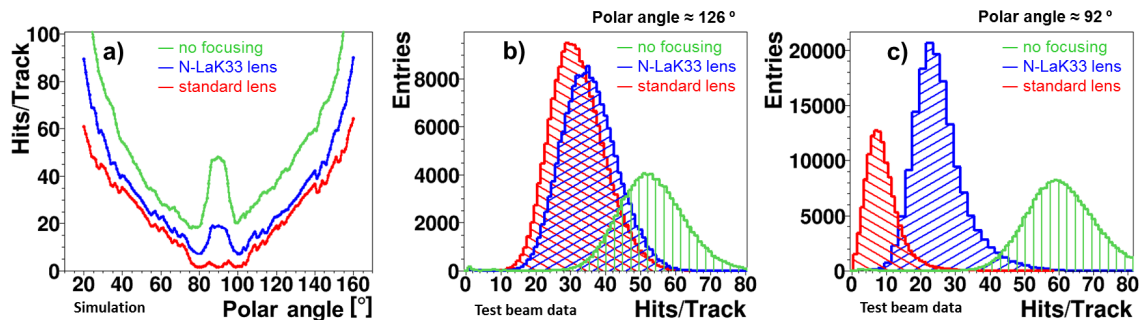


Figure 12. Number of photons per track as a function of polar angle from the prototype ray-tracing simulation (a) for three focusing configurations. Observed number of hits per track from the 2012 prototype for two polar angles and three focusing configurations (b, c). Results for the high-refractive index fused silica/N-LaK33 lens without an air gap are shown in blue, for a standard lens with air gap in red. The configuration without focusing, where the bar is coupled directly to the prism, is shown in green.

The photon yield was measured in the 2012 prototype at CERN for these three types of focusing configurations and two polar angles, one forward angle and one near perpendicular, shown in figure 12b,c. The measured number of hits per track includes contributions from δ electrons (3-5 hits per track) and from charge sharing between MCP-PMT pads (10-15% of the hits), which are not simulated in the ray-tracing software. After correcting for background effects the measured yield is consistent with the prediction from simulation. The performance of the high-refractive index compound lens is quite promising. The higher photon yield makes this design much more tolerant of track and event background than the standard lens with an air gap. An improved version of this lens is being prepared for a test with particle beams in 2014.

A comparison of the narrow bars fabricated using different materials and processes showed that the photon yield for the bar made from acrylic glass was only 20% of the photon yield observed for fused silica bars. Due to the rather short photon paths in this configuration, the measurement was not sensitive enough to bar imperfections to be able to observe significant differences between fused silica bars from different manufacturers. Instead, the high precision measurements from the laser setup will be used to qualify the photon transport efficiency for different prototype bars in the lab.

5 Conclusions

A study of important design elements of the PANDA Barrel DIRC has been carried out using simulation and system prototypes in particle beams. The single photon Cherenkov angle resolution, photon yield, and predicted PID performance were analyzed using a geometric reconstruction method for narrow bars and a time-based likelihood approach for wide radiator plates. Several possible designs were identified which meet the PID performance target of 3 standard deviation π/K separation for up to 3.5 GeV/c momentum. This includes a design using narrow bars and high-refractive index compound lenses without air gap, and a design using wide plates with no focusing elements. Some of these design elements were tested in a particle beam at CERN in 2012. The observed prototype performance was consistent with simulation. More detailed studies, in particu-

lar of the wide radiator plates in combination with focusing optics, and direct measurements of the Cherenkov angle resolution per track, are scheduled for the summer of 2014 during two test beam campaigns at GSI. The results will form the basis for the Technical Design Report, expected to be completed by the end of 2014.

Acknowledgments

This work was supported by HGS-HIRe, HIC for FAIR, EU FP6 grant #515873, EU FP7 grant #227431, and BMBF contract number 05E12CD2. We thank the GSI and CERN staff for the opportunity to use the test beam facilities and for their on-site support.

References

- [1] PANDA collaboration, M. Kotulla et al., *Strong Interaction Studies with Antiprotons*, Technical Progress Report, FAIR-ESAC/Pbar (2005);
PANDA collaboration, M.F.M. Lutz et al., *Physics Performance Report for PANDA: Strong Interaction Studies with Antiprotons*, [arXiv:0903.3905](https://arxiv.org/abs/0903.3905).
- [2] C. Schwarz et al., *Particle identification for the PANDA detector*, *Nucl. Instrum. Meth. A* **639** (2011) 169;
PANDA CHERENKOV collaboration, D. Dutta, *Software development for the PANDA barrel DIRC*, *Nucl. Instrum. Meth. A* **639** (2011) 264.
- [3] BABAR-DIRC collaboration, I. Adam et al., *The DIRC particle identification system for the BaBar experiment*, *Nucl. Instrum. Meth. A* **538** (2005) 281.
- [4] J. Benitez et al., *Status of the Fast Focusing DIRC (fDIRC)*, *Nucl. Instrum. Meth. A* **595** (2008) 104 [INSPIRE].
- [5] C. Field et al., *Development of Photon Detectors for a Fast Focusing DIRC*, *Nucl. Instrum. Meth. A* **553** (2005) 96.
- [6] BELLE II PID collaboration, K. Inami, *TOP counter prototype R&D*, *Nucl. Instrum. Meth. A* **639** (2011) 298;
P. Krizan et al., *Particle Identification at Belle II*, these proceedings.
- [7] Radiant Zemax Europe Ltd., 8 Riverside Business Park, Stoney Common Rd, Stansted, CM24 8PL, U.K., <http://www.zemax.com>.
- [8] GEANT4 collaboration, S. Agostinelli et al., *GEANT4: A Simulation toolkit*, *Nucl. Instrum. Meth. A* **506** (2003) 250;
J. Allison et al., *Geant4 developments and applications*, *IEEE Trans. Nucl. Sci.* **53** (2006) 270;
PANDA collaboration, S. Spataro, *Simulation and event reconstruction inside the PandaRoot framework*, *J. Phys. Conf. Ser.* **119** (2008) 032035;
M. Al-Turany and F. Uhlig, *FairRoot Framework*, *PoS(ACAT08)048*.
- [9] Schott AG, Hattenbergstrasse 10, 55122 Mainz, Germany, <http://www.schott.com>.
- [10] A. Lehmann et al., *Significantly improved lifetime of micro-channel plate PMTs*, *Nucl. Instrum. Meth. A* **718** (2013) 535.
- [11] J. Cohen-Tanugi et al., *Optical properties of the DIRC fused silica Cherenkov radiator*, *Nucl. Instrum. Meth. A* **515** (2003) 680 [hep-ex/0305001].

- [12] M. Staric, *Pattern recognition for the time-of-propagation counter*, *Nucl. Instrum. Meth. A* **639** (2011) 252.
- [13] I. Fröhlich et al., *A General Purpose Trigger and Readout Board for HADES and FAIR-Experiments*, *IEEE Trans. Nucl. Sci.* **55** (2008) 59.
- [14] A. Neiser et al., *TRB3: a 264 channel high precision TDC platform and its applications*, *2013 JINST* **8** C12043.
- [15] F. Anghinolfi et al., *NINO: An ultra-fast and low-power front-end amplifier/discriminator ASIC designed for the multigap resistive plate chamber*, *Nucl. Instrum. Meth. A* **533** (2004) 183;
J. Christiansen et al., *HPTDC High Performance Time to Digital Converter*, CERN-EP-MIC (2004).
- [16] J. Elson, H. Bennett and J. Bennett, *Scattering from Optical Surfaces*, Applied Optics and Optical Engineering Vol. VII, Chapter 7, Academic Press (1979).
- [17] ExxonMobil Lubricants & Specialties Europe, Hermeslaan 2, 1831 Machelen, Belgium,
<http://www.exxonmobil.com>.